IEICE TRANS. COMMUN., VOL.E88–B, NO.11 NOVEMBER 2005

PAPER

Analyzing and Absorbing Cross-Layer Header Overhead of Video Data from End-to-End Viewpoint

Chu-Chuan LEE[†a)], ***Student Member and*** **Pao-Chi CHANG**[††], ***Member***

SUMMARY Regarding IP-based video applications over wireless networks, the multi-layer header overhead may significantly affect the estimation of target video encoding bit rate and the effective throughput of wireless network. Based on the existing header structure of video packets, this study intends to deal with the header overhead problem from the end-to-end viewpoint. This paper first proposes a simple yet robust closed-form that can determine accurately and timely the optimal video payload length at the video sender based on the current wireless channel condition. The contribution can effectively improve the WLAN throughput and enhance the error resilience effect of scalable video data simultaneously. This study further explores the impact of multi-layer header overhead to the video coding work and proposes a Dynamic Header Overhead Accommodation (DHOA) scheme, which is executed in the video compression layer, to adjust dynamically the available video encoding bits for accommodating the header overhead in advance. The contributions of this paper are robust for various IP implementations such as IPSec (IP Security) over different 802.11 standards. Analytical and simulation results verify the accuracy and effectiveness of the proposed closed-form and header accommodation method. Using DHOA, the bandwidth mismatch between the actual bandwidth demand of packetized video data and the available network bandwidth is no more than 1.1% regardless of the packet sizes used in this paper.
key words: *data packetization, video streaming, multimedia application, wireless network*

1. Introduction

With the advances of compression technology and IP network infrastructure, rich IP-based multimedia services, such as real time news, streaming movie, video phone, etc., have dramatically boosted to users [1], [2]. The compressed Variable Bit Rate (VBR) video is one of the major components of most multimedia contents. To enhance the loss and error resilient capabilities of video contents, the Moving Picture Expert Group (MPEG) has developed the MPEG-4 standard to deal with the variable network environment [3]. Regarding the protocol stack at the video sender for transporting the MPEG-4 encoded data, the video compression layer compresses the raw video sequence and generates Elementary Streams (ESs) that contain the coded representation of Visual Objects (VOs). The ESs are packetized as SyncLayer (SL)-packetized streams at the SL. Then, the SL-packetized streams are multiplexed into a FlexMux stream at the TransMux Layer and passed to the transport protocol stack composed of RTP, UDP, and IP [4]. When the IPv6 protocol is used, IPv6 quadruples the number of network address bits from 32 bits of IPv4 to 128 bits and increases the IP header overhead from 20 bytes to 40 bytes [5]. In summary, the multi-layer header overhead of compressed videos includes at least 3 bytes of SL header, 3 bytes of FlexMux header, 16 bytes of RTP header, 8 bytes of UDP header, 20/40 bytes of IPv4/IPv6 header, and the header of selected data link layer, which may affect the estimation of target encoding bit rate of video coding process and the effective throughput of WLAN.

Undoubtedly, the IP world is being extended from wired to wireless infrastructures due to the success of Wireless Local Area Network (WLAN) technologies. Currently, there are three popular IEEE standards available: the Complementary Code Keying (CCK)-based 802.11b [6] in the 2.4 GHz band, the Orthogonal Frequency Division Multiplex (OFDM)-based 802.11a [7] in the 5 GHz band, and the 802.11g [8] based on the same OFDM technology as employed in 802.11a. The 802.11b has the advantage of worldwide spectrum availability while the 802.11a is capable of supporting more high data rate schemes. The 802.11g is formally ratified in June 2003, plus backward compatibility with 802.11b devices. Although the new 802.11e standard holds the promise of Quality of Service (QoS) wherein the network knows to give priority to voice, audio, and video services, the scalability problem of 802.11e for delivering AV contents is still an open issue [9]. Regarding the MAC (Medium Access Control) layer of 802.11b/a/g, there are two access methods: the Distributed Coordination Function (DCF) and the Point Coordination Function (PCF) [10]. The DCF mode is the basic access mechanism that uses the *carrier sense multiple with access/collision avoidance* (CSMA/CA) scheme and the PCF mode is designed for supporting applications that require real-time and contention-free delivery.

Although wireless networks provide users an easy way for accesing audio/video (AV) contents, the received quality is easily affected due to the multipath fading, competing traffic, etc. In wireless networks, ARQ (Automatic Repeat Request) protocols are widely used for error control because they are simple and provide high system reliability. Using proper retransmissions of ARQ can effectively reduce the impact of burst bit-errors to video data. Although video contents are delay sensitive, the latency due to retransmissions is tolerable if a high speed WLAN is used and the retransmission number is properly controlled. On the other

Manuscript received January 24, 2005.
Manuscript revised March 28, 2005.
[†]The author is with the Department of Electrical Engineering, National Central University, Taiwan, R.O.C.
[††]The author is with the Department of Communication Engineering, National Central University, Taiwan, R.O.C.
a) E-mail: chuchu@cht.com.tw
DOI: 10.1093/ietcom/e88–b.11.4360

hand, the Resynchronization Marking (RM) scheme proposed in most video coding standards such as MPEG-4 is generally used to improve the error rresilience capability of video data in the wireless network. However, the determination of optimal video payload length is a cross-layer work. If the RM scheme at the application layer is executed independently, the effective throughput of WLAN may be decreased. This phenomenon is particularly true if the multi-layer header overhead increases or the wireless channel condition changes obviously. Therefore, this paper addresses the above cross-layer work for maximizing the bandwidth utilization and the error resilience effect simultaneously.

There are many research results in this area. In [11], Wright presented and compared different multi-layer header structures of voice data. Although the target of [11] is voice services, video applications have similar problems of header overhead. Schwartz [12] evaluated the throughput efficiency for the ARQ procedure in wireless networks. The analyses of [12] utilized the random bit error model and assumed the permitted retransmission number of ARQ to be infinite for simplifying the analysis process. However, the assumption of infinite ARQ retransmissions is not suitable for delay-sensitive AV contents and the use of random bit error model is not proper to a wireless channel with burst bit-errors. Wu et al. [4] proposed a source rate control mechanism that was adopted by the MPEG-4 standard. A peckatization scheme for MPEG-4 encoded data was also developed. However, the impact of multi-layer header overhead to the actual bandwidth demand of packetized video data at the WLAN MAC layer is not considered and the determination of optimal video payload length associated with the consideration of variable wireless channel conditions is not discussed in [4]. In addition, Modiano [13] proposed a packetization algorithm for wireless networks with the ARQ protocol. However, the determination of optimal packet size only can be obtained by numerical analysis. In [14], Shakkottai et al. addressed the issue of cross-layer networking, where the physical and MAC layer knowledge of the wireless medium could be shared with high layers for providing effective delivery over the Internet. Kumwilaisak et al. [15] proposed a cross-layer quality-of-service (QoS) mapping framework for video transmission in wireless networks. Besides, there are two compression protocols for IP header emerged from the Internet Engineering Task Force (IETF), i.e., the Internet Protocol Header Compression (IPHC) [16] and the Robust Header Compression (ROHC) [17]. IPHC is suitable for links with low bit eror rate (BER) and ROHC is designed for wireless links with high BER. However, high implementation complexity and rare commercial application are the main bottlenecks of ROHC. In addition, regardless of IPHC or ROHC, the header compression requires extra resources on nodes that instantiate the compression algorithm. Therefore, both header compression methods are not included in this paper.

In this paper, we address the multi-layer header overhead problem from the end-to-end viewpoint for delivering video contents over WLANs. This study targets at the PCF (Point Coordination Function) mode of WLAN since it is more approapriate for delay-sensitive AV applications. This paper first formulates a simply yet robust closed-form for determining the optimal video payload length that can maximize the effective throughput of WLAN. The proposed closed-form takes the multi-layer header overhead, the wireless channel condition with burst bit errors, and the finite retransmission number of ARQ into considerations. By comparing these throughput results using different video payload lengths, the throughput degradation is minimized if the optimal video payload length is used. Moreover, we observe that the multi-layer header overhead obviously affects the estimation of target encoding bit rate during the video coding work, particularly when an adaptive packetization scheme with dynamic packet size is used. To solve the above problem, we propose a Dynamic Header Overhead Accommodation (DHOA) scheme, which is executed in the video compression layer, to adjust dynamically the available video encoding bits for accommodating the multi-layer header overhead in advance. Notably, the contributions are robust for various IP implementations such as IPSec over different 802.11 b/a/g standards.

This paper is constructed as follows. In Sect. 2, we present the theoretical analyses for achieveing the maximum effective throughput of 802.11b/a/g networks. A closed-form of optimal video payload length is formulated. In Sect. 3, operations of the proposed DHOA scheme are described in details. In Sect. 4, we validate the numerical results by comparing with simulation results. Finally, Sect. 5 concldes this paper.

2. Theoretical Analyses of Optimal Video Packet Size

For formulating the optimal video payload length in WLAN environment, we utilize the Gilbert model [18] to characterize the error sequences generated by wireless channel, as plotted in Fig. 1. From [18] the average bit error rate of Gilbert model can be expressed as

$$p_{be} = \frac{a}{\alpha + \beta} \tag{1}$$

and the burst error length, b, also can be given by

$$b = \frac{1}{\beta} \tag{2}$$

Meanwhile, considering a video packet with P bits of encoded video data and H_{CL} bits of multi-layer header overhead, this study formulates the average packet error rate

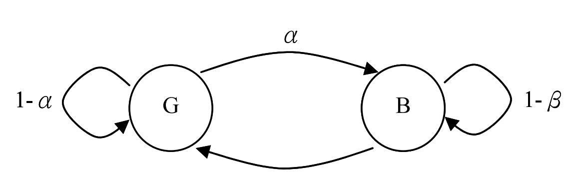

Fig. 1 Gilbert model.

(PER) in a wireless channel with burst bit errors as

$$p_{pe} = 1 - \{[P(G|B) \cdot P(B) + P(G|G) \cdot P(G)] \cdot (1-\alpha)^{P+H_{CL}-1}\} \quad (3)$$

By substituting (1) into (3) and evaluating (3), we have

$$\begin{aligned} p_{pe} &= 1 - \left\{\left[\frac{(1-\alpha)\cdot\beta}{\alpha+\beta} + \frac{\alpha\cdot\beta}{\alpha+\beta}\right] \cdot (1-\alpha)^{P+H_{CL}-1}\right\} \\ &= 1 - \left[(1-p_{be})\cdot(1-\alpha)^{P+H_{CL}-1}\right] \end{aligned} \quad (4)$$

If L_r is the permitted maximum retransmission number for a video packet over a wireless channel with p_{be}, the probability that the packet is successfully delivered within L_r retransmission limit is computed as

$$\begin{aligned} p_{s-L_r} &= (1-p_{pe}) + (1-p_{pe})\cdot p_{pe} + \cdots + (1-p_{pe})\cdot p_{pe}^{L_r} \\ &= \left(1 - p_{pe}^{L_r+1}\right) \end{aligned} \quad (5)$$

In other words, the probability that the delivery for the packet is not successful after L_r retransmission limit is given by

$$p_{f-L_r} = p_{pe}^{L_r+1} \quad (6)$$

Consequently, the mean transmission number that a video packet is successfully delivered within L_r retransmission limit is calculated by

$$\begin{aligned} S_{succ} &= 1\cdot\frac{(1-p_{pe})}{p_{s-L_r}} + 2\cdot\frac{p_{pe}\cdot(1-p_{pe})}{p_{s-L_r}} + \cdots + (L_r+1)\cdot\frac{p_{pe}^{L_r}\cdot(1-p_{pe})}{p_{s-L_r}} \\ &= \frac{1}{p_{s-L_r}}\cdot\{(1-p_{pe}) + 2\cdot\left[(1-p_{pe})\cdot p_{pe}\right] + \cdots + (L_r+1)\cdot\left[p_{pe}^{L_r}\cdot(1-p_{pe})\right]\} \\ &= \frac{1}{\left(1-p_{pe}^{(L_r+1)}\right)}\cdot\frac{1}{(1-p_{pe})}\cdot \left\{\left(1-p_{pe}^{(L_r+1)}\right) - (L_r+1)\cdot p_{pe}^{(L_r+1)} \cdot(1-p_{pe})\right\} \end{aligned} \quad (7)$$

The mean transmission number for a video packet with the limit of L_r retransmissions is then given by

$$\begin{aligned} S_{avg} &= (S_{fail}\cdot p_{f-L_r}) + (S_{succ}\cdot p_{s-L_r}) \\ &= [(L_r+1)\cdot p_{f-L_r}] + (S_{succ}\cdot p_{s-L_r}) \end{aligned} \quad (8)$$

From normal operations of WLAN, the duration of a successful cycle, i.e., neither the video data packet nor the ACK packet is in error, can be computed as

$$T_{s-cyc} = T_{data} + 2\cdot T_{SIFS} + T_{ack} \quad (9)$$

where T_{data} and T_{ack} are the transmission times for delivering a video data packet and a ACK packet, respectively. That is,

$$T_{data} = T_{PHY} + \left(\frac{P+H_{CL}}{R}\right) \quad (10)$$

$$T_{ack} = T_{PHY} + \left(\frac{8\cdot 14}{R}\right) \quad (11)$$

or

$$\begin{aligned} T_{data} &= T_{PHY} + T_{SYM}\cdot\left\lceil\frac{16+6+P+H_{CL}}{N_{DBPS}}\right\rceil \\ &\cong T_{PHY} + \left(\frac{22+P+H_{CL}}{R}\right) \\ &= T_{PHY} + C_{PHY} + \left(\frac{P+H_{CL}}{R}\right) \end{aligned} \quad (12)$$

$$\begin{aligned} T_{ack} &= T_{PHY} + T_{SYM}\cdot\left\lceil\frac{16+6+8\cdot 14}{N_{DBPS}}\right\rceil \\ &\cong T_{PHY} + \left(\frac{22+8\cdot 14}{R}\right) \\ &= T_{PHY} + C_{PHY} + \left(\frac{8\cdot 14}{R}\right) \end{aligned} \quad (13)$$

where

R : transmission rate of WLAN.
T_{PHY} : required time that transmits the preamble bits and the header of WLAN physical layer.
T_{SYM} : required time for transmitting a symbol in IEEE 802.11a or IEEE 802.11g-OFDM.
N_{DBPS}: bits that contained in the symbol.

In addition, the length of an ACK packet is 14 bytes and the 22 bits in (12) and (13) is the partial header of IEEE 802.11a or IEEE 802.11g-OFDM physical layer that locateded in the payload field. Note that Eqs. (10) and (11) are applied to the case of IEEE 802.11b or IEEE 802.11g-CCK and Eqs. (12) and (13) are applied to the case of IEEE 802.11a or IEEE 802.11g-OFDM. Similarly, the duration of a failure cycle i.e., either the video data packet or the ACK packet is in error, can be calculated by

$$T_{f-cyc} = T_{data} + T_{PIFS} \quad (14)$$

where the duration of a failure transmission due to an erroneous ACK packet is assumed to be the same as that due to an erroneous video data packet for simplifying the analysis. The difference between two failure transmission durations is very little.

Assuming that the delivery of video packets is a sequence of independent Bernoulli trials, the expected number of Bernoulli trials until the first successful video packet is received by the station is just the reciprocal of (5) and expressed as

$$N_P = \frac{1}{p_{s-L_r}} = \frac{1}{\left(1-p_{pe}^{L_r+1}\right)} \quad (15)$$

Now, from the station viewpoint, the average time interval between two correctly received video packets can be computed by

$$T_{total} = (N_P \cdot S_{avg} - 1) \cdot T_{f-cyc} + T_{s-cyc} \tag{16}$$

By substituting (4), (8) and (15) into (16) and evaluating (16), we have

$$\begin{aligned} T_{total} &= N_P \cdot S_{avg} \cdot \left\{ \frac{P + H_{CL}}{R} + C_{PHY} + T_{PHY} \right. \\ &\quad \left. + T_{PIFS} \right\} + 2 \cdot T_{SIFS} + T_{ack} - T_{PIFS} \\ &= N_P \cdot S_{avg} \cdot \left(\frac{P + H_{CL}}{R} + C_1 \right) + C_2 \\ &= \frac{1}{(1-\alpha)^{P+H_{CL}-1}} \cdot \left\{ \left(\frac{P + H_{CL}}{R} + C_1 \right) \right. \\ &\quad \left. \cdot \frac{1}{(1 - p_{be})} + (1-\alpha)^{P+H_{CL}-1} \cdot C_2 \right\} \end{aligned} \tag{17}$$

where C_{PHY} is set to zero if the IEEE 802.11b or IEEE 802.11g-CCK is used.

In the saturated transmission case, the maximum throughput of WLAN, in packets/sec delivered, is just the reciprocal of T_{total}. The effective throughput D_e, in bits/sec delivered, is then given by

$$\begin{aligned} D_e(P) &= \frac{1}{T_{total}} \cdot P = P \cdot (1-\alpha)^{P+H_{CL}-1} \\ &\quad \div \left\{ \frac{1}{1 - P_{be}} \cdot \left(\frac{P + H_{CL}}{R} + C_1 \right) \right. \\ &\quad \left. + C_2 \cdot (1-\alpha)^{P+H_{CL}-1} \right\} \triangleq \frac{f(P)}{g(P)} \end{aligned} \tag{18}$$

By differentiating Eq. (18) with respect to P and setting the derivative to 0, we have

$$f(P) \cdot g'(P) = f'(P) \cdot g(P) \tag{19}$$

where

$$\begin{aligned} f'(P) &= (1-\alpha)^{P+H_{CL}-1} \\ &\quad + P \cdot (1-\alpha)^{P+H_{CL}-1} \cdot \ln(1-\alpha) \end{aligned} \tag{20}$$

$$\begin{aligned} g'(P) &= \frac{1}{R \cdot (1 - p_{be})} \\ &\quad + (1-\alpha)^{P+H_{CL}-1} \cdot C_2 \cdot \ln(1-\alpha) \end{aligned} \tag{21}$$

By substituting (20) and (21) into (19) and evaluating (19), we have

$$\begin{aligned} &\frac{P}{R \cdot (1 - p_{be})} \\ &\quad + (1-\alpha)^{P+H_{CL}-1} \cdot P \cdot C_2 \cdot \ln(1-\alpha) \\ &= [1 + P \cdot \ln(1-\alpha)] \\ &\quad \cdot \left\{ \frac{1}{1 - p_{be}} \cdot \left(\frac{P + H_{CL}}{R} + C_1 \right) \right. \\ &\quad \left. + (1-\alpha)^{P+H_{CL}-1} \cdot C_2 \right\} \end{aligned} \tag{22}$$

After further evaluating (22), we obtain

$$\begin{aligned} &C_4 \cdot (1-\alpha)^P + \ln(1-\alpha) \cdot P^2 \\ &\quad + C_3 \cdot \ln(1-\alpha) \cdot P + C_3 = 0 \end{aligned} \tag{23}$$

where

$$C_3 = H_{CL} + R \cdot C_1 \tag{24}$$

$$C_4 = (1-\alpha)^{H_{CL}-1} \cdot R \cdot (1 - p_{be}) \cdot C_2 \tag{25}$$

Meanwhile, we extend the item $(1-\alpha)^P$ of (23) as

$$\begin{aligned} (1-\alpha)^P &= 1 - \alpha \cdot P + \alpha^2 \cdot \frac{P!}{2! \cdot (P-2)!} \\ &\quad - \alpha^3 \cdot \frac{P!}{3! \cdot (P-3)!} + \cdots \end{aligned} \tag{26}$$

For simplifying the analyses and obtaining a closed-form, we ignore the later items of (26) whose power of P exceeds two. Then, Eq. (26) can be simplified as

$$(1-\alpha)^P \cong 1 - \alpha \cdot P + \alpha^2 \cdot \frac{1}{2} \cdot P \cdot (P-1) \tag{27}$$

By substituting (27) into (23) and evaluating (23), we have

$$\begin{aligned} &\left[\frac{1}{2} \cdot \alpha^2 \cdot C_4 + \ln(1-\alpha) \right] \cdot P^2 \\ &\quad + \left[C_3 \cdot \ln(1-\alpha) - C_4 \cdot \left(\alpha + \frac{1}{2} \cdot \alpha^2 \right) \right] \\ &\quad \cdot P + (C_3 + C_4) = 0 \end{aligned} \tag{28}$$

Finally, the optimal value of P that maximizes the effective throughput D_e can be calculated from (28) and is given as

$$P_{opt} = \frac{C_6 - \sqrt{C_6^2 - 2 \cdot C_7 \cdot (C_3 + C_4)}}{C_7} \tag{29}$$

where

$$\begin{aligned} C_5 &= \frac{C_4 \cdot \left[(1-\alpha)^2 - 4 \cdot (1-\alpha) + 3 \right]}{2} \\ &= C_4 \left(\alpha + \frac{1}{2} \cdot \alpha^2 \right) \end{aligned} \tag{30}$$

$$C_6 = C_5 - C_3 \cdot \ln(1-\alpha) \tag{31}$$

$$C_7 = \alpha^2 \cdot C_4 + 2 \cdot \ln(1-\alpha) \tag{32}$$

From (29), we can easily and timely determine the optimal video payload length based on the current wireless channel condition. Whenever the optimal payload length is determined, the RM scheme at the application layer adopts the optimal payload length to packetize the video data and the packetization mechanisms at other layers are also based on the same optimal payload length plus the required headers. The contribution also can be applied to an adaptive packetization mechanism where the dynamic packet size strategy is used for coping with variable wireless channel conditions. Moreover, regarding different IP implementations such as IPSec, tunneling mechanism, etc., we also can easily obtain the impact of header overhead to WLAN throughput by means of (29).

3. Accommodation of Variable Header Overhead

This paper assumes that the available network bandwidth for a new connection is negotiated and determined in the call setup stage by means of proper signaling and bandwidth allocation techniques such as Asynchronous Transfer Mode (ATM) [19] or Resourse ReSerVation Protocol (RSVP) [20]. After determining the available network bandwidth, the estimation of target encoding bit rate is based on the given network bandwidth directly. In general, the multi-layer header overhead is not taken into consideration in the estimation procedure. This may cause the mismatch between the available network bandwidth and the actual bandwidth demand of the encoded video. Besides, the overall header overhead of a video sequence is variable when an adaptive packetization strategy with dynamic packet size is used for overcoming dynamic wireless channel conditions. The variable header overhead may further worsen the bandwidth mismatch problem and thus increase the complexity of resource management and the loss/delay possibility of video data. To solve above problems, this work proposes the DHOA scheme, which is executed in the video compression layer, to adjust dynamically the available video encoding bits for accommodating the multi-layer header overhead in advance.

In this section, a discrete-time model with the unit of frame number is used. At the beginning of the video coding process with DHOA, the target encoding bit rate is set to the available network bandwidth directly. When the video encoder finishes the encoding operation for the current video frame f_n at time n, DHOA computes the required multi-layer header overhead H_n for packetizing the encoded bits of f_n by

$$H_n = H_{CL} \cdot \left\lceil \frac{A_n}{P_n} \right\rceil \tag{33}$$

where A_n is the encoded bits of f_n and P_n is the optimal payload length calculated by (29). Clearly, the value of H_n increases if a small payload length is used or the value of H_{CL} is enlarged. Notably, the value of P_n may be variable if an adaptive packetization mechanism is activated for overcoming the variable network condition such as WLAN.

Now, DHOA takes the header overhead H_n of f_n into consideration while encoding the next video frame f_{n+1}. When the encoding procedure for f_{n+1} begins, the target encoding bits for f_{n+1} is estimated by the following improved expression

$$R_{n+1} = \frac{B_{n+1} - H_n}{u_{n+1}} \cdot (1 - S) + A_n \cdot S \tag{34}$$

where

B_{n+1}: remaining available bits for the video sequence at time $n + 1$.

R_{n+1}: target encoding bits for the video frame f_{n+1}.

u_{n+1}: remaining raw video frames which are not encoded yet at time $n+1$.

S : weighting factor to determine the impact of the previous frame on the calculation of target encoding bits. The value is set to 0.05 in our experiments.

From (34), the header overhead H_n of f_n is subtracted from the remaining available bits B_{n+1} before determining the target encoding bits of f_{n+1}. Repeating the procedure, the required multi-layer header overhead of each video frame is automatically accommodated into the budget of available encoding bits of the video sequence. When DHOA is used, the delivered IP-based video traffic can accurately match the available bandwidth that the network can provide. The contribution is robust even an adaptive packetization mechanism with dynamic packet size strategy is activated and is independent of the infrastructure of networks. Moreover, when the bit rate of medium is dynamically changed due to the variable wireless channel condition, DHOA still can solve the problem effectively. When the video encoder receives the feedback information of new available network bandwidth from AP, the difference between the two successive network bandwidths is subtracted from or added to the remaining available bits B_{n+1} directly, and the consequent operation of DHOA for f_{n+1} is the same as before. However, although DHOA can support the dynamic transmission rate of WLAN, a stable provision of network bandwidth is significantly helpful to the received picture quality from the viewpoint of video services.

4. Numerical Results and Discussions

This study constructs two WLAN simulation environments, 802.11g and 802.11b, to verify the accuracy of the formulated closed-form and to evaluate the impact of multi-layer header overhead to WLAN throughput and video coding work. The architecture of the simulation testbed is plotted in Fig. 2 in which each module is implemented by C++. Regarding the video sender, this study uses the MPEG-4 RM-18 codec [3] to generate the compressed video sequences and the proposed mechanism is implemented here. The video sequences are CIF format with the frame rate of 30 fps. Considering the AP, the PCF mode is activated and a Deficit Round Roubin (DRR) scheduler is implemented. The quantum value of DRR is set to 2500 bytes that is larger than the maximum MAC frame size of 802.11 and

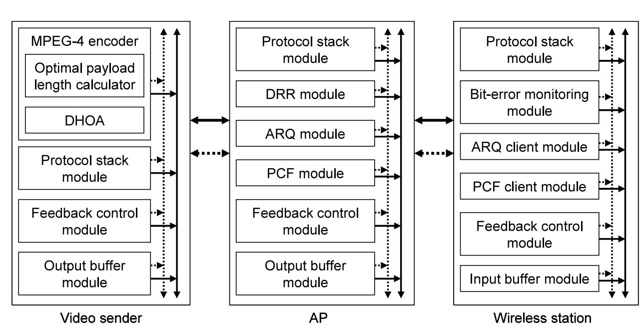

Fig. 2 The architecture of simulation test-bed.

Table 1 Parameters of 802.11b/a/g.

	802.11b	802.11a	802.11g OFDM/CCK
Progressing Delay	$1\,\mu s$	$\ll 1\,\mu s$	$\ll 1\,\mu s$
$T_{H\text{-}PHY}$	$48\,\mu s$	$4\,\mu s$	$4\,\mu s/48\,\mu s$
Preamble Time ($T_{preamble}$)	$144\,\mu s$	$16\,\mu s$	$16\,\mu s/144\,\mu s$
Time Slot(T_{slot})	$20\,\mu s$	$9\,\mu s$	$9\,\mu s/20\,\mu s$
Short IFS(T_{SIFS})	$10\,\mu s$	$16\,\mu s$	$16\,\mu s/10\,\mu s$
PCF IFS(T_{PIFS})	$30\,\mu s$	$25\,\mu s$	$25\,\mu s/30\,\mu s$
DCF IFS(T_{DIFS})	$50\,\mu s$	$34\,\mu s$	$34\,\mu s/50\,\mu s$

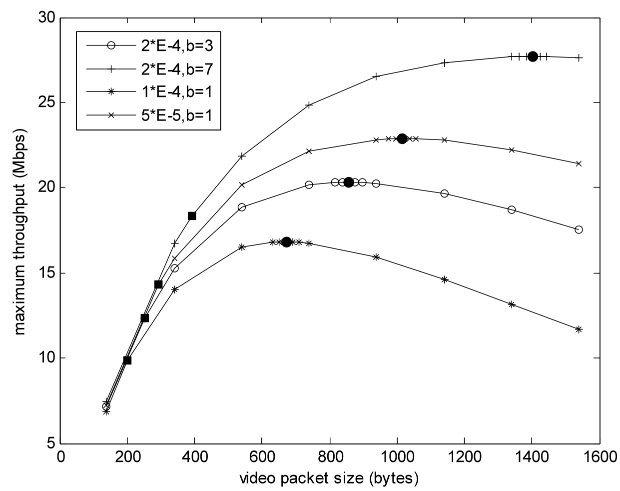

Fig. 3 IPv4 video packet sizes versus 802.11g throughputs under different BERs and burst error lengths.

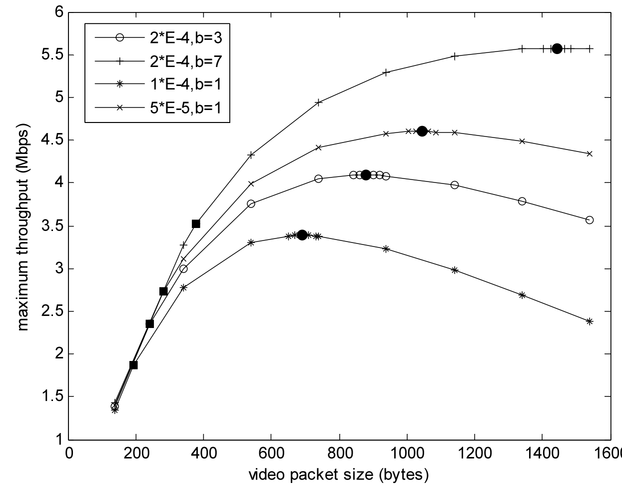

Fig. 4 IPv4 video packet sizes versus 802.11b throughputs under different BERs and burst error lengths.

the queue length in AP is assumed to be infinite. This work assumes that the OFDM technique is used in the physical layer of 802.11g and that the bandwidth of 802.11g is set to 54 Mbps. The results of 802.11a network are not presented in this section since its performances and parameters are similar to the case of 802.11g with OFDM technique. These used parameter values of 802.11b/a/g are presented in Table 1. We use the Gilbert model to simulate various wireless channel conditions. The values of α and β can be directly determined by Eqs. (1) and (2), i.e., $\alpha = BER/(b - b \cdot BER)$ and $\beta = 1/b$. Three BERs, $2{\cdot}E$-4, $1{\cdot}E$-4 and $5{\cdot}E$-5, associated with three burst error lengths, 1, 3 and 7, are used to generate different wireless channel conditions. Regarding the simulation scenarios, an AP with a single wireless station that requests the video streaming service is considered. In following discussions, all results shown in the figures are calculated by averaging the outcomes that are obtained from fifty simulation runs with different random seeds.

Figure 3 first shows 802.11g throughputs versus IPv4 video packet sizes under different BERs and burst error lengths. Herein a traditional solution of [12] is compared with the proposed closed-form. To explore the maximum throughput of 802.11g, a pre-stored video data file is continuously deliveried to a wireless station. By means of simulation results, we plot a convex curve and find an optimal video packet size that maximizes the WLAN throughput for each wireless channel condtiion. On the other hand, we use the proposed closed-form to obtain the analytically optimal video packet size for each wireless channel condition. These analytical results are plotted in Fig. 3 by shaded circles. Similarly, the analytical results computed by the traditional closed-form of [12] are also plotted by shaded squares. From Fig. 3 we observe that the analytically optimal packet size calculated by the proposed closed form and the simulation result are in good agreement in each wireless channel condition, where the maximum difference is less than 10 bytes. This verifies the accuracy of the closed-form formulated by this paper. How-ever, when the traditional closed-form of [12] is used, we find that the difference between the analytically optimal packet size and the simulated optimal packet size is up to 1011 bytes in the case of $2{\cdot}E$-4 with $b = 7$. The main reason is that the given closed-form of [12] is based on the assumptions that the bit error model is random and the permitted retransmission number of ARQ is infinite.

Figure 4 uses the same simulation conditions except that 802.11g is replaced by 802.11b. From Fig. 4 we obtain similar conclusions for the proposed method among the video packet size, the BER and the throughput. Herein we also observe that the throughput in the case of long burst error length is larger than that of short burst error length under the same BER. The main reason is that this study uses the ARQ approach as the major error control approach. When the ARQ tech-nique is used for a specified BER, the PER with short burst error length is higher than that with long burst error length. These results of Fig. 4 also exhibit that the proposed closed-form is robust for various 802.11 WLAN standards.

Figures 5 and 6 further evaluate the impact of header increase of IPv4 IPSec strategy to 802.11g and 802.11b throughputs with different BERs and burst error lengths. When the IPSec protocol is used, the header overhead of network layer may increase double compared to existing IP header overhead. In this simulation scenario, we consider

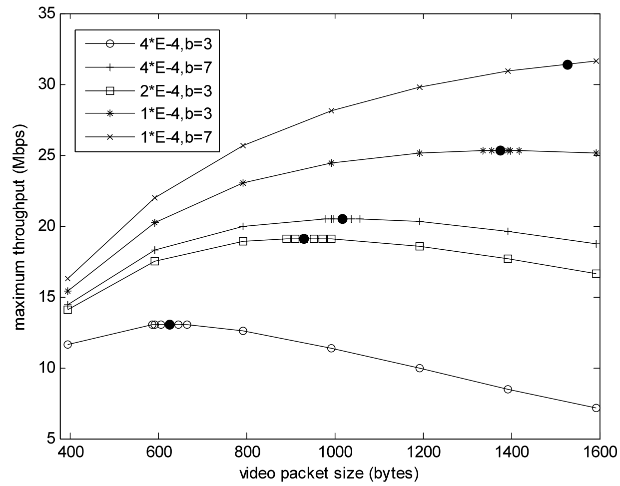

Fig. 5 IPv4 IPSec packet sizes versus 802.11g throughputs under different BERs and burst error lengths.

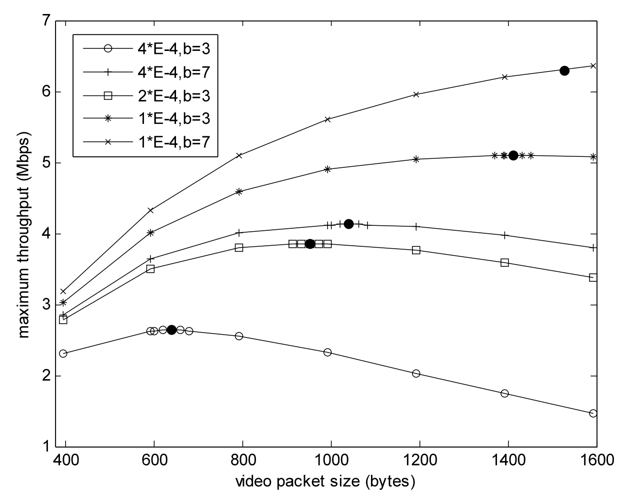

Fig. 6 IPv4 IPSec packet sizes versus 802.11b throughputs under different BERs and burst error lengths.

the Authentication Header (AH) protocol with tunnel mode. In the tunnel mode, the entire original datagram is regarded as the payload, and a newly created outer IP header and an AH header are added to the original data datagram. By comparising the results of Figs. 5 and 6 with that of Figs. 3 and 4, we find that the throughput of 802.11g degrades up to 1.1 Mbps in the case of $2{\cdot}E$-4 with $b = 3$ due to the header increase of IPv4 IPSec packets. These results also exhibit that the proposed closed-form is robust for various IP implements.

Finally, this work explores the effectiveness of DHOA, as presented in Fig. 7. This paper uses the MPEG-4 encoder to generate a standard test sequence "*Foreman*" and uses four different video packet sizes for discussion. The available network bandwidth is assumed to be 1 Mbps and the target encoding bit rate is set to 1 Mbps based on the available network bandwidth directly. For explanation, the actual bandwidth demand of packetized video

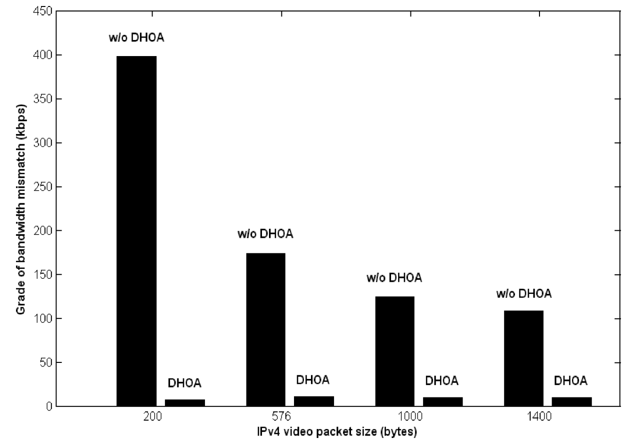

Fig. 7 Mismatch between the available network bandwidth and the actural bandwidth demand for delivering *Foreman*.

data and the available network bandwidth at the MAC layer of WLAN are denoted as BW_{dem} and BW_{ava}, respectively. Meanwhile, considering the video coding work without DHOA, the bandwidth mismatch, defined as $BW_{mis} = [(BW_{dem} - BW_{ava}) \cdot 100\%] / BW_{ava}$, is up to 39.8% for a short packet size of 200 bytes. This mismatch is mainly due to the header overhead. Fortunately, when the proposed DHOA method is activated, the bandwidth mismatch is no more than 1.1% for all packet sizes examined in the simulation. The contribution of DHOA is robust to various video packet sizes and the header overhead of each video packet is automatically and accurately accommodated into the video coding process. No coarse bandwidth reservation for header overhead is required in the stage of determining the target encoding bit rate.

5. Conclusion

This paper proposes a simple yet robust closed-form that can: 1) determine accurately and timely the optimal video payload length at the video sender according to the current wireless channel status; 2) quantify effectively the WLAN throughput degradation due to the header increase of various IP implementations; 3) enhance effectively the error resilience effect of scalable video data. Moreover, this paper also proposes an effective DHOA mechanism that can accommodate dynamically and accurately the header overhead of video packets during the video coding process. When DHOA is activated, the bandwidth mismatch between the actual bandwidth demand of packetized video data and the available network bandwidth is no more than 1.1% for all packet sizes examined in this study. No coarse bandwidth reservation for header overhead is required in the stage of determining the target encoding bit rate.

References

[1] K.A. Hua, M.A. Tantaoui, and W. Tavanapong, "Video delivery technologies for large-scale deployment of multimedia applications," Proc. IEEE, vol.92, no.9, pp.1439–1451, Sept. 2004.

[2] S.M. Faccin, P. Lalwaney, and B. Patil, "IP multimedia services: Analysis of mobile IP and SIP interactions in 3G networks," IEEE Commun. Mag., vol.42, no.1, pp.113–120, Jan. 2004.
[3] ISO/IEC JTC1/SC29/WG11, "MPEG-4 video verification modelversion 18.0," N3908, Jan. 2001.
[4] D. Wu, Y.T. Hou, W. Zhu, T.H. Chiang, Y.Q. Zhang, and H.J. Chao, "On end-to-end architecture for transporting MPEG-4 video over the Internet," IEEE Trans. Circuits Syst. Video Technol., vol.10, no.6, pp.923–941, Sept. 2000.
[5] P. Cocquet, "IPv6 on DSL: The best way to develop always-on services," Proc. IEEE, vol.92, no.9, pp.1400–1407, Sept. 2004.
[6] IEEE 802.11, "Part 11: Wireless LAN medium access control (MAC) and physical layer (PHY) specifications: High-speed physical layer extension in the 2.4 GHz band," IEEE Standard, Sept. 1999.
[7] IEEE 802.11, "Part 11: Wireless LAN medium access control (MAC) and physical layer (PHY) specifications: High-speed physical layer in the 5 GHz band," IEEE Standard, Sept. 1999.
[8] IEEE 802.11, "Part 11: Wireless LAN medium access control (MAC) and physical layer (PHY) specifications: Amendment 4: Further higher data rate extension in the 2.4 GHz band," IEEE Standard, June 2003.
[9] E. Griffith, "Don't wait for 802.11e," Available: http://www.wi-fiplanet.com/news/article.php/3088611
[10] J.H. Yeh, J.C. Chen, and C.C. Lee, "WLAN standards," IEEE Potentials, vol.22, no.4, pp.16–22, Oct./Nov. 2003.
[11] D. Wright, "Voice over MPLS compared to voice over other packet transport technologies," IEEE Commun. Mag., vol.40, no.11, pp.124–132, Nov. 2002.
[12] M. Schwartz, Telecommunication Networks: Protocols, Modeling and Analysis, pp.119–135, Addison-Wesley, 1987.
[13] E. Modiano, "An adaptive algorithm for optimizing the packet size used in wireless ARQ protocols," Wirel. Netw., vol.5, no.4, pp.279–286, May 1999.
[14] S. Shakkottai and T.S. Rappaport, "Cross-layer design for wirless networks," IEEE Commun. Mag., vol.41, no.10, pp.74–80, Oct. 2003.
[15] W. Kumwilaisak, T. Hou, Q. Zhang, W. Zhu, C.-C.J. Kuo, and Y.Q. Zhang, "A cross-layer quality-of-service mapping architecture for video delivery in wireless networks," IEEE J. Sel. Areas Commun., vol.21, no.10, pp.1685–2003, Dec. 2003.
[16] M. Degermark, B. Nordgren, and S. Pink, "IP header compression," IETF RFC 2507, Feb. 1999.
[17] C. Bormann, C. Burmeister, M. Degermark, H. Fukushima, H. Hannu, L.-E. Jonsson, R. Hakenberg, T. Koren, K. Le, Z. Liu, A. Martensson, A. Miyazaki, K. Svanbro, T. Wiebke, T. Yoshimura, and H. Zheng, "Robust header compression (ROHC): Framework and four profiles: RTP, UDP, ESP, and uncompressed," IETF RFC 3095, July 2001.
[18] J.R. Yee and E.J. Weldon, Jr., "Evaluation of the performance of error-corresting codes on a Gilbert channel," IEEE Trans. Commun., vol.43, no.8, pp.2316–2323, Aug. 1995.
[19] T.V. Lakshman, P.P. Misbra, and K.K. Ramakrishnan, "Transporting compressed video over ATM networks with explicit rate feedback control," IEEE/ACM Trans. Netw., vol.7, no.5, pp.710–723, Oct. 1999.
[20] R. Braden, L. Zhang, S. Berson, S. Herzog, and S. Jamin, "Resource reservation protocol (RSVP)," IETF RFC 2205, Sept. 1997.

Chu-Chuan Lee received the B.S. and M.S. degrees in Electrical Engineering from National Taiwan University of Science and Technology, Taiwan, in 1990 and 1992, respectively, and the Ph.D. degree from National Central University, Taiwan, 2005. Since 1992, he has been working as a Researcher at the Chunghwa Telecommunication Laboratories (CHTTL), Taiwan. At CHTTL, his work centers on multimedia over IPv4/IPv6 networks, migration from IPv4 to IPv6, and planning of broadband metro/core networks. His research interests include scalable video coding, IPv4/IPv6 transitioning, and smooth delivery of videos over wired/wireless networks.

Pao-Chi Chang received the B.S. and M.S. degrees from National Chiao Tung University, Taiwan, in 1977 and 1979, respectively, and the Ph.D. degree from Stanford University, California, 1986, all in electrical engineering. From 1986 to 1993, he was a research staff member of the department of communications at IBM T.J. Watson Research Center, Hawthorne, New York. At Watson, his work centered on high speed switching systems, efficient network design algorithms, and multimedia conferencing. In 1993, he joined the faculty of National Central University, Taiwan, where he is presently a Professor in the Department of Communication Engineering. His research interests include speech/audio coding, video/image compression, scalable coding, error resilient coding, digital watermarking and data hiding, and video delivery over packet and wireless networks. He has published more than 70 journal and conference papers in these areas.